A docking system for microsatellites based on MEMS actuator arrays

Mason Terry[1]**, Joel Reiter**[1]**, Karl F Böhringer**[1]**, John W Suh**[2] **and Gregory T A Kovacs**[3]

[1] Department of Electrical Engineering, University of Washington, Seattle, WA 98195, USA
[2] Systems and Practices Laboratory, Xerox Palo Alto Research Center, Palo Alto, CA 94304, USA
[3] Center for Integrated Systems, Department of Electrical Engineering, Stanford University, Stanford, CA 94305, USA

Abstract
Microelectromechanical system (MEMS) technology promises to improve performance of future spacecraft components while reducing mass, cost, and manufacturing time. Arrays of microcilia actuators offer a lightweight alternative to conventional docking systems for miniature satellites. Instead of mechanical guiding structures, such a system uses a surface tiled with MEMS cilia actuators to guide the satellite to its docking site.

This paper summarizes work on an experimental system for precision docking of a 'picosatellite' using MEMS cilia arrays. Microgravity is simulated with an aluminum puck on an airtable. A series of experiments is performed to characterize the cilia, with the goal of understanding the influence of normal force, picosatellite mass, docking velocity, cilia actuation frequency, interface material, and actuation strategy ('gait') on the performance of the MEMS docking system.

We demonstrate a 4 cm^2 cilia array capable of docking a 41.2 g picosatellite with a 2 cm^2 contact area with micrometer precision. It is concluded that current MEMS cilia arrays are effective in positioning and aligning miniature satellites for docking to a support satellite.

(Some figures in this article are in colour only in the electronic version)

1. Introduction

A number of microelectromechanical system (MEMS) cilia systems have been developed with the common goal of moving and positioning small objects, so far always under the force of gravity. Similar to biological cilia, all of these systems rely on many actuators working in concert to accomplish the common goal of transporting an object of muchlarger size than each individual cilium. Recent techniques range from air jets [1–3], electromagnetic actuators [4–6], piezoelectric actuators [7], single-crystal silicon electrostatic actuators [8, 9], thermal-bimorph (bimaterial) actuators [10–13], to electrothermal (single-material) actuators [14, 15]. In parallel, researchers have studied the control of distributed microactuation systems and cilia arrays [16–22].

The goal of this project is to investigate the feasibility of a MEMS-based space docking system. For such a system, the docking approach is divided into two phases: (1) free flight and rendezvous, with the goal of achieving physical contact between the two satellites, and (2) precision docking with the goal of reaching accurate alignment between the satellites (e.g. to align electrical or optical interconnects). Phase 1 constitutes unconstrained motion with 6 degrees of freedom and lower accuracy for the rendezvous; phase 2 constitutes planar motion with 3 degrees of freedom and high accuracy. The MEMS-based approach for phase 2 represents the key innovation in this project. Therefore, the investigation of MEMS cilia as a means to achieve precise alignment between two satellites represents the primary focus of this paper. To demonstrate a complete system-level solution, phase 1 was investigated as well [23] but will not be discussed here.

During this project thermally actuated polyimide based microcilia, as seen in figure 1 and identical to those described in [13], are characterized to ascertain their practicality for docking miniature spacecraft. To this end, experiments were performed using an airtable (see figure 2) which is designed to
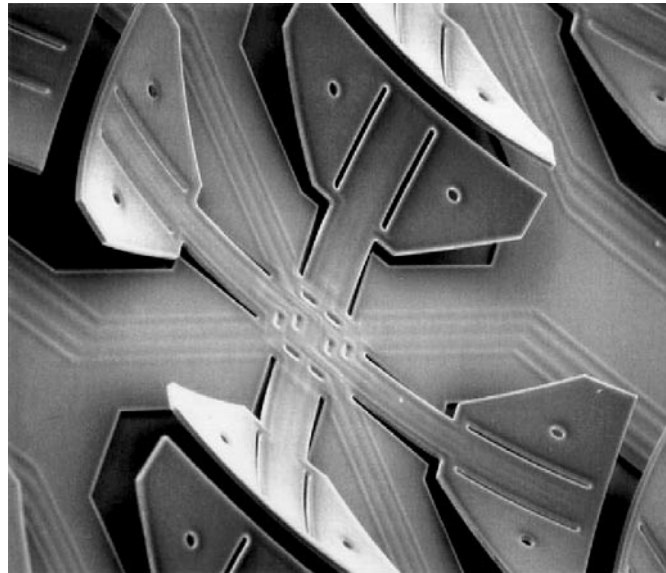
Figure 1. Scanning electron microscope (SEM) view of a single microcilia motion cell. The cell is approximately 1 mm long and wide (image by John Suh (1997)).
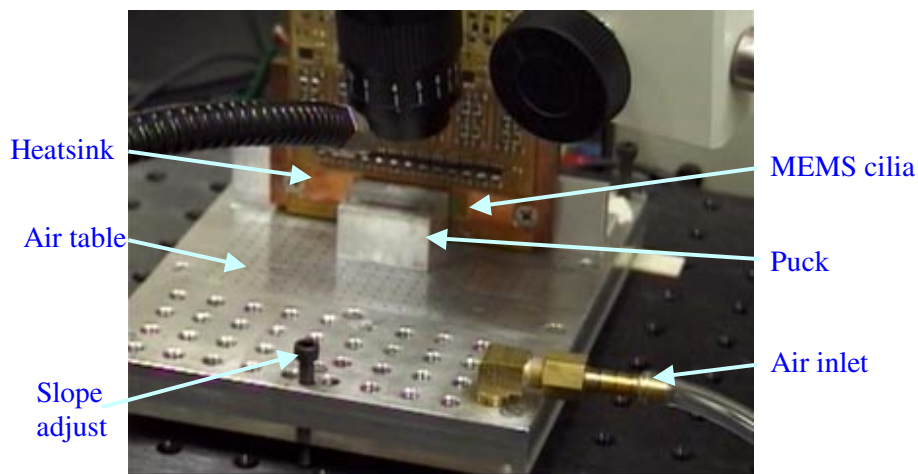

Figure 2. Airtable experimental setup to simulate microsatellite docking. An $8'' \times 6''$ perforated aluminum plate with 3 adjustable support screws provides levitation support for an aluminum puck ('picosat'). Microcilia chips are mounted on a vertical copper plate with heat sink.

support the microcilia in a vertical configuration. A rectangular aluminum block referred to as a puck, which has a mass between 40 and 45 g, is used to simulate a picosatellite. The airtable can be tilted towards the microcilia, producing a known normal force against the faces of the chips. This force can then be adjusted independently from the mass of the simulated picosatellite. To increase the realism of the experiment and to ease data collection, position sensing and position feedback are incorporated and computer controlled. Two position-sensing systems are used: an array of Hall effect sensors and a video-capture-based system. These are strictly non-contact techniques compatible with a space environment.

Next we describe the experiments that were performed with the microcilia with the goal of evaluating the appropriateness of microcilia to spacecraft docking applications. Four different materials (polished ceramic; polystyrene; smooth aluminum and silicon, both rough and polished) were used for the cilia-to-puck interface surface. Interestingly, polished ceramic

achieved the highest puck velocities of all the interfaces and polished silicon attained higher velocities than rough silicon.

Through the course of this study microcilia were able to provide the speed, robustness, reliability and strength for use in miniature spacecraft applications. The microcilia successfully moved blocks of aluminum in excess of 40 g mass and calculations indicate that a patch of cilia 25 cm in radius would be sufficient to position a 40 kg satellite.

2. Micro- and picosatellites

The adoption of the 'faster–better–cheaper' paradigm has resulted in increasing interest in so-called microsatellites (mass 1–100 kg) and picosatellites (mass <1 kg). One important future task for micro- and picosatellites, hereafter referred to as just microsatellites, is inspecting a larger satellite for damage. Figure 3 describes a large, broad purpose satellite surrounded by a constellation of smaller, mission-specific satellites. The
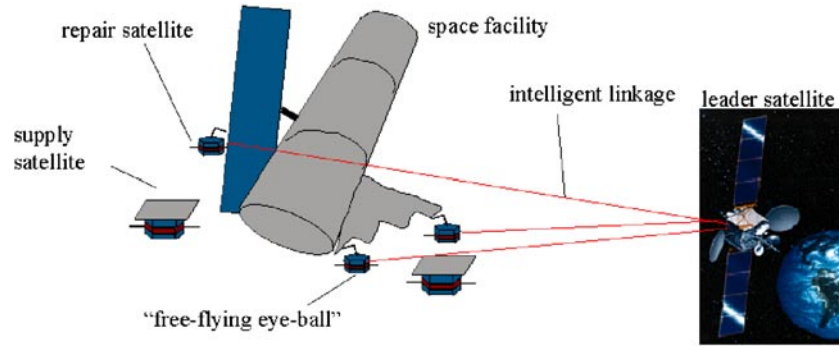
Figure 3. Envisioned microsatellite mission [23]. Picosatellites (mass <1 kg) are used for routine inspection and repair of a space station.
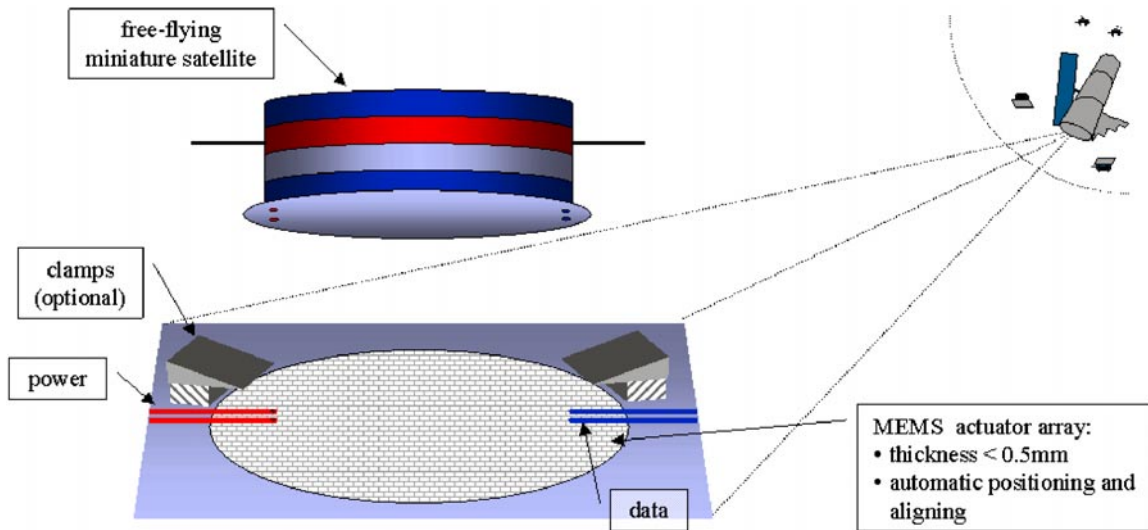

Figure 4. Conceptual cilia picosatellite docking application. The docking site of the space station is covered with a micro-actuator array that provides for precision alignment of the microsatellite to power and data lines.

miniature satellites provide inspection, maintenance, assembly and communication services for their larger brethren. Cameras mounted on the microsatellites provide imagery of the primary platform that is otherwise unobtainable. From these pictures, damage could be assessed and the mission of the main satellite adapted. Due to their simplicity, small size, weight and limited interaction with ground controllers these specialized satellites are expected to be indispensable during future missions [23].

As the size of satellites shrink, their ability to carry fuel and power is reduced. It is expected that this will force microsatellites to dock frequently to replenish their resources. Since the time spent docking reduces the microsatellites' mission time, this procedure should be as simple and quick as possible. When docking microspacecraft there are two primary tasks: attaching the microsatellite to the larger craft, and orienting the satellite to connect fuel, data and electrical services. The first docking task is largely the domain of the microsatellite and is dependent on how quickly velocity adjustments can be made, and on the specific attachment mechanism. The second phase of docking is dependent on the speed at which the satellite can be positioned to connect electrical and other services. Figure 4 shows the conceptual cilia application for space docking of miniature satellites. A surface on the mother satellite is covered with cilia actuators that will position the microsatellite for refueling and data transfer.

3. Experimental setup

The measurements in this paper are performed using the thermal-actuator-based microcilia (see again figure 1) originally described by Suh *et al* [13]. A cross section of a microcilium arm is shown in figure 5. The arrayed actuators are deformable microstructures that curl out of the substrate plane. The curling of the actuators is due to the different coefficients of thermal expansion (CTE) of the polyimide layers that make up the bimorph structures. For these devices the top layer CTE is greater than the bottom CTE. The thermal stress from this interface causes the actuator to curl away from the substrate at low temperatures and towards it when heated. The displacement of the microcilia arm relative to its location before release both vertically, δ_V, and horizontally, δ_H, is given by

$$\delta_V = R \left(1 - \cos\left(\frac{L}{R}\right)\right) \tag{1}$$

$$\delta_H = L - R \sin\left(\frac{L}{R}\right) \tag{2}$$

where R (≈ 800 μm) is the radius of curvature and L (≈ 430 μm) is the length of the actuator which results in a horizontal displacement of $\delta_H = 20$ μm and vertical
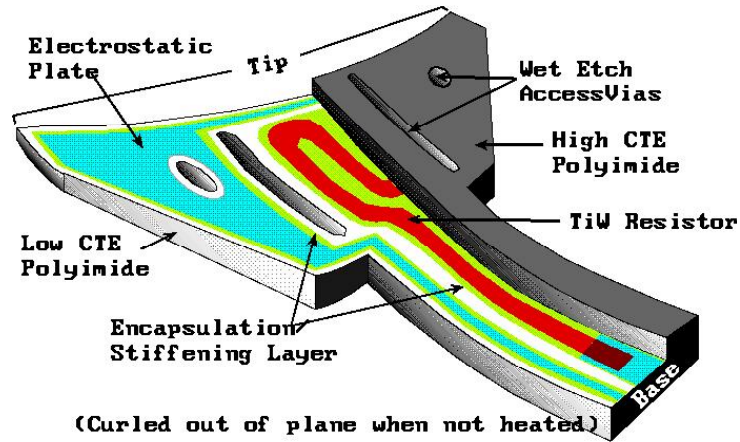
Figure 5. Cross sectional view of the cilia with two layers of polyimide, titanium–tungsten heater loop, silicon nitride stiffening layer, and aluminum electrostatic plate (image by John Suh (1997)).

displacement of $\delta_V = 114$ μm. A detailed description of the cilia actuators and their operation was given in [12, 13].

An array of cilia is configured in an 8×8 motion cell layout within a 1 cm^2 die. Each motion cell contains four orthogonally oriented actuators within an area of 1.1 mm $\times$ 1.1 mm (see again figure 1). A control line independently actuates each actuator of the motion cell. All actuators oriented in the same direction in each motion cell are controlled together. They are electrically connected in series in every column of the chip, and all columns are connected in parallel[4].

The microcilia arm is placed into motion using a titanium–tungsten heating resistor that is sandwiched between two silicon nitride and two polyimide layers. When a current is passed through this loop, the temperature of the actuator increases, and the structure deflects downward. This produces both horizontal and vertical displacements at the tip of the microcilia. Typical drive conditions were 40–60 V and 20–30 mA peak currents at frequencies up to 60 Hz.

Objects in contact with the surface of the array are made to move by coordinating the deflections of many actuators. Next we describe how the cilia are controlled with gait-like patterns to produce motion. These gaits consist of multiple states (phases) that alternate repeatedly. For this study, three- and four-phase gaits are used during interface experiments and normal force experiments. For the four-phase gait the motions of the microcilia arms correspond to those shown in figure 6. This motion gait has four phases, during which two transitions produce forward motion.

The sequence of phases starts with both arms flattened. The left (west) arm is released, forcing the object up and to the east. Next, the right (east) arm is released which rises to make contact with the object. Then the west arm is pulled down, leaving the east actuator to support the object. The final phase and start of a new phase in the sequence results in the object moving down and to the east. The three-phase gait is the same as the four-phase except the phase at the top of figure 6 is skipped; instead the east arm is released and the west arm is pulled down simultaneously.

To assess the applicability of microcilia to spacecraft docking this study investigates the effects of operating

---

[4] Therefore, the total nominal resistance R of each control line is equal to the resistance R_c of an individual actuator cilium: $R = (8 \cdot R_c)/8$.
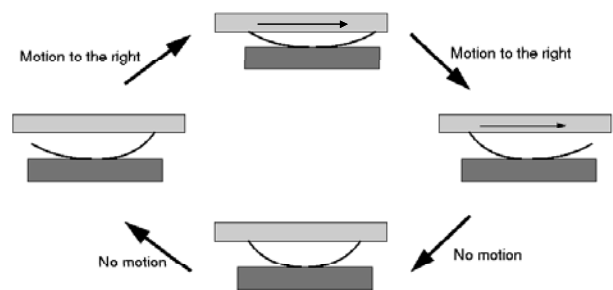

Figure 6. The four-phase cilia motion gait showing the actuation sequence to produce motion towards the right (east).

frequency, normal force, interface surfaces, microcilia temperature, and, indirectly, microcilia life span. Of these variables, frequency and life span depend directly on the thermal actuation nature of the cilia while the remaining parameters should be applicable to other types of MEMS microactuator arrays, too. To perform measurements the microcilia are placed vertically at the end of a tilted airtable as shown in figures 7 and 8. A $31.6 \times 24.4 \times 18.9$ mm^3 aluminum block, referred to as a puck, is used to simulate a satellite. The mass of the puck varied between 41 and 45 g, depending on the specifically mounted interface surface. The table is first leveled and then the angle adjustment is slightly manipulated to specify a slope running towards the microcilia. By adjusting the slope of the table, the mass of the aluminum puck can remain fixed while a variable normal force is applied against the microcilia. Conversely, the mass of the puck can be varied while the normal force against the microcilia is kept constant. Using this parameter independence, the airtable allows for an accurate simulation of microsatellite docking in microgravity. With this setup, the microcilia can manipulate objects that would otherwise flatten the actuators if all the gravitational force were applied as the normal force.

This experiment uses four microcilia chips attached to a copper block that both actively cools the microcilia using a Peltier junction and holds them vertical at the end of the airtable. The microcilia chips were glued into a groove machined in the copper block, forcing all four chips to lie in the same plane in a horizontal linear array.
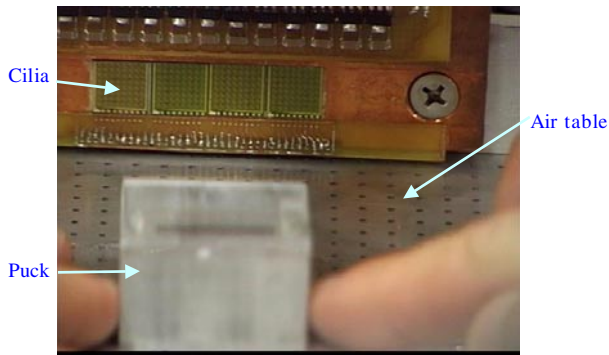
Figure 7. Close-up view of cilia and airtable showing the puck in the foreground. Index fingers in foreground give a size reference. When the puck is released it slides on the slightly inclined airtable towards the MEMS cilia, simulating the rendezvous phase of microsatellite docking.
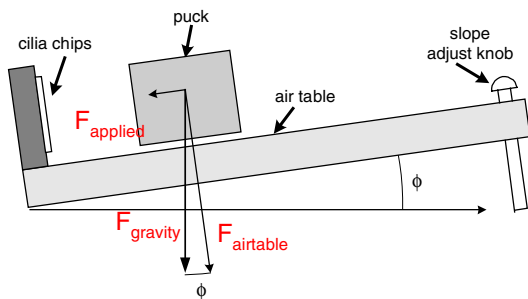

Figure 8. Schematic side view of the airtable (not to scale, and slope exaggerated).

During all of the experiments the microcilia were controlled with the LabView interface seen in figure 9 and custom circuitry. Each of the microcilia gaits is broken down into a statemachine describing the sequence of movements for each of the microcilia arms. This statemachine is then loaded into an LSI programmable gate array, one per microcilia chip. The LabView interface instructs the LSI chips which gait to use, the direction to travel and the frequency through which to cycle the cilia gait. LabView also reads the Hall effect sensor array output and from that data controls the starting and ending points of the puck motion.

To make displacement measurements two separate systems are employed. The first is a high-resolution video capture system. This system, equipped with a zoom lens, allows for relative measurements in the order of 5 μm and for capturing expanded views of the system. A video capture and distance measurement system has been developed to better characterize the cilia motion. The image of the puck is captured using a CCD camera mounted on a variable zoom, 1–10, microscope. This image is then converted to a black and white image for feature tracking using Matlab.

The other measurement system is an array of Hall effect sensors. These sensors interact with a magnet mounted atop the puck to provide micrometer resolution. This system has a passive part, the magnet, that can be viewed as a benefit to space applications. The Hall effect sensor array is integrated into the LabView controlling software, allowing fully automated experiments to be performed. Using either of these systems it

is possible to collect the relative puck position and from this to compute the velocity and acceleration of the puck.

4. Experimental results

The goal of this research is to evaluate the applicability of MEMS cilia arrays to microsatellite docking. Thermal bimorph microcilia arrays [12, 13] are parameterized for operating frequency, normal force, puck mass, interface surfaces, cilia temperature and cilia lifespan. The results for these experiments are presented here.

4.1. Effects of normal force

Figure 10 shows the velocity of the puck at different frequencies over two different normal forces. For all of these data points the mass of the puck is 41.2 g and the interface surface is a 0.9 cm $\times$ 2.5 cm piece of polystyrene, beveled on the edges. Each data point is an average of four runs over a distance of 0.8 mm using a four-phase gait. A polynomial fit is used for the trend line.

Over a range of about 5–30 Hz the puck velocity increases approximately proportionally to the drive frequency[5]. This characteristic indicates the interface between the puck and microcilia arms is experiencing a small, fixed slip component. At these frequencies the puck motion seems largely the result of a 'step and carry' transport. The graph also indicates that the overall velocity of the puck increases as the normal force against the cilia surface decreases to a minimum normal force value. This is an expected result because, as the normal force increases, so does the precompression of the cilia, reducing their total vertical and horizontal motion. This implies that the optimal normal force is that where the puck exerts just sufficient force to maintain contact with the cilia surface.

4.2. Effects of interfacing surfaces

Differences between thermal conduction and surface roughness of the puck to the microcilia interface affects step size and puck velocity. The five puck-to-microcilia interface materials examined are polished ceramic, hard polystyrene plastic beveled on the ends, aluminum, and polished and unpolished silicon. Puck velocity versus actuation frequency for the different interface materials is shown in figures 11 and 12 for three- and four-phase gaits, respectively. Actuation frequency is defined as the completion of a full cycle of actuation where the three-phase gait encompasses three distinct phases and the four-phase gait is composed of four distinct phases. Puck velocity is obtained by averaging a minimum of five trials per frequency with a normal force of 63 μN mm^{-2}. The distance the puck traveled for these measurements varies between 0.1 and 0.6 mm with increasing actuation frequency. A polynomial fit is applied to all data points.

When comparing the different interface materials as shown in figures 11 and 12 it can be observed that the materials with the lowest thermal conduction provide the

---

[5] There exist, however, two regions at frequencies between 13 and 16 Hz, and between 30 and 33 Hz, where the graph deviates from this pattern. Experimental observations indicate that this is due to resonances of the mass–spring–damper system represented by the puck, normal force, and flexible MEMS cilia. This resonance is discussed in more detail below.
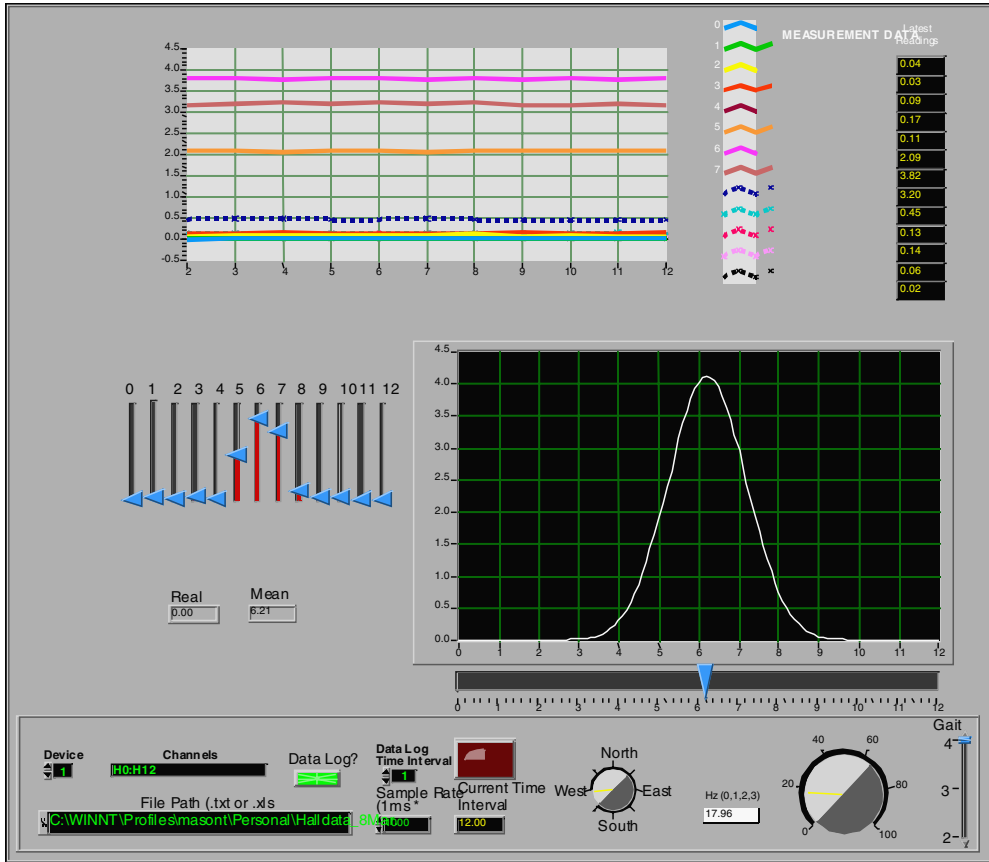
Figure 9. LabView interface for the microcilia. Top and left: sensor readings from Hall effect array. Right: Gaussian curve fit and puck position. Bottom: MEMS cilia array controller for direction, actuation frequency, and gait selection.
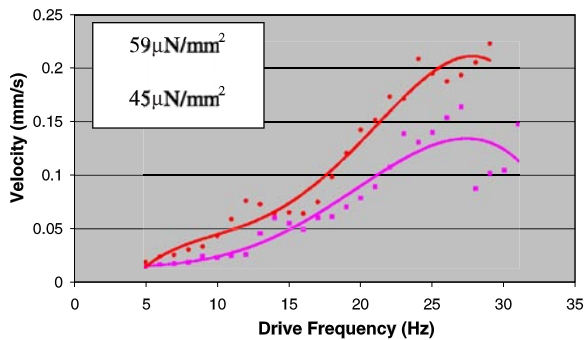

Figure 10. The velocity of the airtable puck (using the beveled plastic interface) versus different drive frequencies as a function of normal forces.

highest velocities. Aluminum and silicon have the highest thermal conduction and this results in the lowest velocities. Ceramic, an excellent thermal and electrical insulator, delivers some of the highest velocities. Low thermal conduction of the ceramic interface allows the cilia to heat and cool in an optimal fashion, resulting in high actuation amplitudes and high puck velocities. The thermal conduction of the interface material is thought to be the major cause for the variation in velocity magnitude per material. The polystyrene interface has non-ideal thermal effects when interfaced with the cilia. Heat from the cilia is transmitted to the polystyrene surface, which is subsequently softened. This softening allows the cilia to form

small indentations, which remain once the cilia are removed from the interface during the next actuation cycle.

As summarized in figure 13, the velocity of the puck is dependent on the roughness of the material interfaced with the microcilia. Polished silicon realizes higher puck velocities for both the three- and four-phase gaits. This is thought to be the result of higher surface uniformity and contact area between the cilia and interface. A rough surface could allow greater slippage between the cilia and interface due to a lower contact surface area. Additionally, a rough surface can interfere with the cilia actuation due to the surface 'catching' the cilia during actuation.

Missing data points in the three-phase graph and the flatter areas of the other graphs are due to the puck oscillating with zero or reduced velocity for multiple trials at the specific frequency. This effect is distributed over the entire cilia experimental surface. The neighborhoods of 17.5 and 33 Hz show the most pronounced reduction in puck velocity for both gaits and all interface materials. The variation of this effect for different surface material and puck mass indicates that it is strongly dependent upon the specific parameters of the experiment. It is thought that this phenomenon can be traced partly to the puck breaking contact with the microcilia surface during part of the motion cycle. As the normal force is increased, this effect becomes less pronounced: however, it is still consistently observed. Within these frequency bands the puck was observed to intermittently move away from the cilia surface by up to 100 μm, in accordance with this explanation.
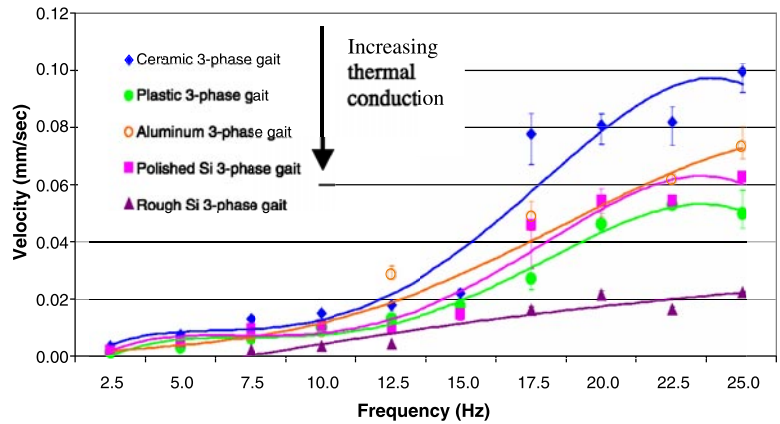
1181

Figure 11. Influence of interface material on puck velocity using a three-phase gait.
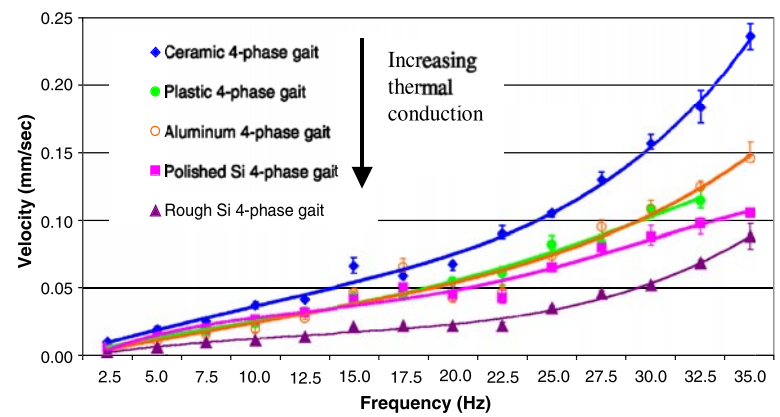

Figure 12. Influence of interface material on puck velocity using a four-phase gait.
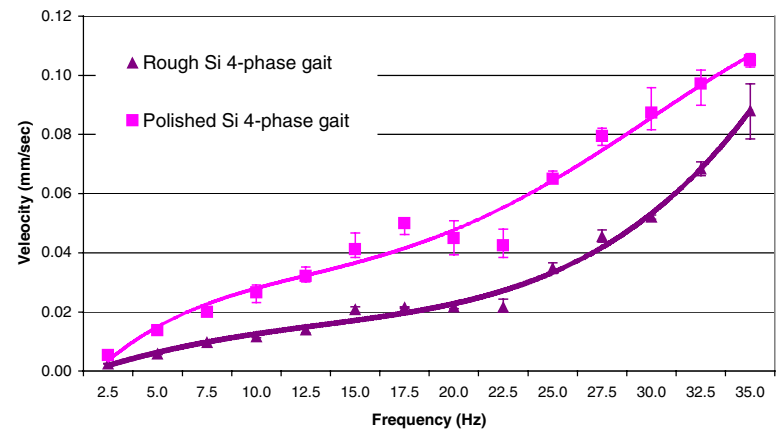

Figure 13. Comparison of both rough and polished silicon interface for both three- and four-phase gaits.

4.3. Thermal effects

As the background temperature of the microcilia is allowed to increase the actuators become less effective. With rising background temperature the change in cilia temperature from rest, ΔT, is smaller. As such, the total displacement of the cilia tip from rest to full deflection decreases. In the extreme case the background temperature becomes large enough that the heater loop cannot raise the temperature of the cilia higher than the background. At this background temperature, no heating period would be sufficient to allow the cilia to have a net displacement. Objects in contact with the cilia would no longer be transported at this point.

This scenario was experimentally verified. If the polarity of the Peltier junction that normally cools the microcilia is reversed, it provides active heating as opposed to active cooling. As the background temperature of the cilia increases their actuation displacement decreases. Eventually all visible movement halts. Once this point is reached the heater is turned off and the microcilia are allowed to cool.

The cooling of the cilia is a negative exponential decay that approaches ambient temperature asymptotically. As the frequency of actuation increases, the time the cilia have to cool decreases. Once the cooling time becomes sufficiently small, the cilia temperature can no longer approach room temperature. Further increases in actuation frequency result in the minimum cooling point on the negative exponential curve to increase until the cooling temperature is equal to the actuation temperature maximum. This effect is similar to a capacitor that is given an ever-decreasing discharge time between maximum charges. The initial few actuations of the cilia are observed to have larger tip displacements than subsequent actuations because the cilia have had sufficient time to cool to room temperature initially. As the frequency of actuation is increased, the tip displacement decreases gradually.

4.4. Lifespan

Over the course of these experiments the microcilia were shown to be robust and the results reproducible. Four chips, corresponding to 4×256 actuators, were run for approximately 180 h at an average of 25 Hz. This corresponds to 16.2 million actuations per cilia actuator or a total of 16.6 billion total actuations. The cilia were designed for a nominal resistance of 1.5 kΩ [13]; actual resistance varied between 1.2 and 3.0 kΩ. Voltages up to 60 V were applied to the network of 8 parallel $\times$ 8 serial cilia for each motion direction on a chip, resulting in a peak power dissipation of approximately 20 mW per cilium (3 kΩ at 60 V; or 1.2 kΩ at 40 V). In a motion gait, the duty cycle of a cilium is 1/2 or 1/3 of an entire period (for four-phase or three-phase gaits, respectively; see again figure 6). Therefore, the average power dissipation is 6.7–10 mW for an individual cilium, or 1.7–2.6 W for the entire chip. We estimate the peak temperature to be approximately 300 °C, which was sufficiently high to cause localized melting of contacting polystyrene surfaces and charring of paper.

During the entire test time only one microcilium actuator leaf was lost. This failure was in an individual heater loop and probably corresponded to a local thickening of the material or contaminants in that area during manufacture. Subsequent checks of other microcilia, under standard operating conditions, could determine no mechanical or electrical faults.

However, prolonged operation at elevated temperatures can eventually damage the actuators. Possible failures include fusing of the heater wire and charring of the polyimide. Localized charring over some heating loops was observed and is shown in figure 14. This charring was confined to 70% of actuators on one chip and resulted from driving at extremely high temperatures. No significant charring was seen on the other seven tested chips.

5. Conclusions

The results from these experiments indicate that a microcilia surface can be useful for docking small spacecraft. These spacecraft, used for inspection, maintenance, assembly and communication services, will see increased use in space missions and become more autonomous and far reaching [23]. During this scenario, microcilia provide a good match,
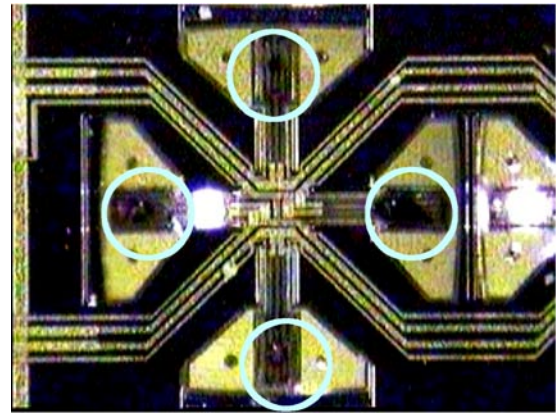

Figure 14. Localized charring of polyimide surface above heater loop.

allowing for simple docking procedures to be used with these simple satellites.

Results from the interface experiments indicate that a variety of materials common to spacecraft can be used as docking surfaces including aluminum and silicon, thus avoiding the need for special materials on the mating surfaces. When studying the performance of different interface materials, thermal conduction dominates surface roughness to achieve optimal object velocity. Surface roughness does affect object velocity as seen in the polished and unpolished silicon. An interface material, such as ceramic, with low thermal conduction and little surface roughness should be selected for an optimal docking surface although aluminum has been shown to be a good second choice.

Using microcilia to perform the delicate final orientation and positioning of the satellite may greatly speed up the docking operation because the entire satellite, with its fixed connections, could be mated to fixed connections on the main satellite. This alleviates the use of flexible and cumbersome umbilical cords and attendant positioning systems.

A further benefit of using microcilia as a docking surface is a reduction in mass compared to other docking and alignment techniques. On the host satellite only a surface of microcilia is required along with minimal control electronics and sensors. The microcilia docking system could simply replace one of the satellite's body panels for maximum weight saving. On the microsatellite side, the additional mass needed to incorporate docking functionality could be as low as zero. The optimal microcilia interface is a flat plane, which may already be part of the microsatellite chassis, thus requiring minimal integration.

The microcilia themselves have inherent advantages for this application. Foremost among these advantages is their ability to arbitrarily position the satellite anywhere on the surface and in any orientation. The microcilia can also act as sensors: however, it has already been demonstrated that they can position objects open loop with little loss of accuracy [18]. By using thousands of microcilia on a single docking patch, it is possible to build systems that incorporate massive redundancy. Thus, if there is some kind of docking mishap the entire mission need not be affected. Finally, thermal microcilia have been shown to perform better in vacuum than air [24]. This is largely due to a lack of convective cooling which slows the heating cycle.

The scalability of microcilia also enables the construction of widely varied systems. While the primary task envisioned for microcilia is manipulating picosatellites (mass <1 kg), much greater masses are feasible. By using additional cilia and a greater contact area, larger satellites can be handled. The current generation of microcilia is capable of moving a 41.2 g puck with an interface area of 2 cm^2. This indicates that a patch only 25 cm in radius (1000 times as large as the area in the experiment) would be sufficient to position satellites with more than 40 kg mass under microgravity conditions.

Through the course of this study the microcilia exhibited the speed, robustness, reliability and strength needed for this application. These results show that microcilia can be an attractive alternative to conventional docking systems for microsatellite applications.

Acknowledgments

References

[1] Pister K S J, Fearing R and Howe R 1990 A planar air levitated electrostatic actuator system *Proc. IEEE 5th Workshop on Micro Electro Mechanical Systems (Napa Valley, CA, Feb. 1990)* pp 67–71

[2] Konishi S and Fujita H 1994 A conveyance system using air flow based on the concept of distributed micro motion systems *J. Microelectromech. Syst.* **3** 54–8

[3] Mita Y, Konishi S and Fujita H 1997 Two-dimensional micro conveyance system with through holes for electrical and fluidic interconnection *Transducers '97 Dig. 9th Int. Conf. on Solid-State Sensors and Actuators (IEEE) (Chicago, IL, June 1997)* vol 1 pp 37–40

[4] Liu C, Tsai T, Tai Y-C, Liu W, Will P and Ho C-M 1995 A micromachined permalloy magnetic actuator array for micro robotics assembly systems *Transducers '95 Dig. 8th Int. Conf. on Solid-State Sensors and Actuators/Eurosensors IX (IEEE) (Stockholm, Sweden, June 1995)* vol 1 pp 328–31

[5] Liu W and Will P Parts manipulation on an intelligent motion surface *Proc. 1995 IEEE/RSJ Int. Conf. on Intelligent Robots and Systems (IEEE) (Pittsburg, PA, Aug. 1995)* vol 3 pp 399–404

[6] Nakazawa H, Watanabe Y and Morita O 1997 The two-dimensional micro conveyor: principles and fabrication process of the actuator *Transducers '97 Dig. 9th Int. Conf. on Solid-State Sensors and Actuators (IEEE) (Chicago, IL, June 1997)* vol 1 pp 33–6

[7] Furihata T, Hirano T and Fujita H 1991 Array-driven ultrasonic microactuators *Transducers '91 Dig. 6th Int. Conf. on Solid State Sensors and Actuators (IEEE) (San Francisco, CA, June 1991)* pp 1056–9

[8] Böhringer K-F, Donald B R and MacDonald N C 1996 Single-crystal silicon actuator arrays for micro manipulation tasks *Proc. IEEE 9th Workshop on Micro Electro Mechanical Systems (MEMS) (San Diego, CA, Feb. 1996)* pp 7–12

[9] Böhringer K-F, Donald B R and MacDonald N C 1999 Programmable vector fields for distributed manipulation, with applications to MEMS actuator arrays and vibratory parts feeders *Int. J. Robot. Res.* **18** 168–200

[10] Takeshima N and Fujita H 1991 Polyimide bimorph actuators for a ciliary motion system *ASME WAM, Symp. on Micromech. Sensors, Actuators, and Systems DSC* vol 32 pp 203–9

[11] Ataka M, Omodaka A and Fujita H 1993 A biomimetic micro motion system *Transducers '93 Dig. 7th Int. Conf. on Solid State Sensors and Actuators (IEEE) (Pacifico, Yokohama, Japan, June 1993)* pp 38–41

[12] Suh J W, Glander S F, Darling R B, Storment C W and Kovacs G T A 1996 Combined organic thermal and electrostatic omnidirectional ciliary microactuator array for object positioning and inspection *Tech. Dig. Solid-State Sensors and Actuator Workshop Transducers Research Foundation (Hilton Head, SC, June 1996)* pp 168–73

[13] Suh J W, Glander S F, Darling R B, Storment C W and Kovacs G T A 1997 Organic thermal and electrostatic ciliary microactuator array for object manipulation *Sensors Actuators* A **58** 51–60

[14] Ebefors T, Mattsson J U, Kèlvesten E and Stemme G 1999 A robust micro conveyor realized by arrayed polyimide joint actuators *Proc. IEEE 12th Workshop on Micro Electro Mechanical Systems (MEMS) (Orlando, FL, Jan. 1999)* pp 576–81

[15] Kladitis P E, Bright V M, Harsh K F and Lee Y C 1999 Prototype microrobotics for micro positioning in a manufacturing process and micro unmanned vehicles *Proc. IEEE 12th Workshop on Micro Electro Mechanical Systems (MEMS) (Orlando, FL, Jan. 1999)* pp 570–5

[16] Fujita H 1993 Group work of microactuators *Int. Adv. Robot Program Workshop on Micromachined Technologies and Systems (Tokyo, Japan, Oct. 1993)* pp 24–31

[17] Böhringer K, Donald B, Mihailovich R and MacDonald N C 1994 A theory of manipulation and control for microfabricated actuator arrays *Proc. IEEE MEMS '94 (Oiso, Japan, Jan. 1994)*

[18] Liu W and Will P 1995 Part manipulation on an intelligent motion surface *IEEE/RSJ Int. Workshop on Intelligent Robots and Systems (IROS) (Pittsburg, PA, Aug. 1995)* vol 3 pp 399–404

[19] Böhringer K, Suh J, Donald B and Kovacs G 1997 Vector fields for task-level distributed manipulation: experiments with organic micro actuator arrays *Proc. 1997 IEEE Int. Conf. on Robotics and Automation* vol 2 pp 1779–86

[20] Böhringer K-F, Donald B R and MacDonald N C 1999 Programmable vector fields for distributed manipulation, with applications to MEMS actuator arrays and vibratory parts feeders *Int. J. Robot. Res.* **18** 168–200

[21] Mita Y, Kaiser A, Stefanelli B, Garda P, Milgram M and Fujita H 1999 A distributed microactuator conveyance system with integrated controller *Proc. IEEE SMC '99* vol 1 pp 18–21

[22] Böhringer K-F and Howie Choset 2000 *Distributed Manipulation* (Dordrecht: Kluwer) pp 272

[23] Campbell M and Böhringer K 1999 Intelligent satellite teams for space systems *Proc. 2nd Int. Conf. on Integrated Micro/Nanotechnology for Space Applications* vol 2 pp 193–204

[24] Darling R, Suh J and Kovacs G 1998 Ciliary microactuatory array for scanning electron microscope positioning stage *J. Vac. Sci. Technol.* A **16** 1998–2002